

24
-22-80

MASTER

SAND79-0224
Unlimited Release

AN AUTOMATED ELECTRONIC INTRUDER SIMULATOR
FOR EVALUATION OF ULTRASONIC INTRUSION DETECTORS

DEPARTMENT 1720



Sandia Laboratories

SF 2900 Q17-73

DISTRIBUTION OF THIS DOCUMENT IS UNLIMITED

SAND79-0224
Unlimited Release
Printed January 1979

AN AUTOMATED ELECTRONIC INTRUDER SIMULATOR
FOR EVALUATION OF ULTRASONIC INTRUSION DETECTORS

Information Systems Department 1730
Sandia Laboratories
Albuquerque, NM 87185

ABSTRACT

An automated electronic intruder simulator for testing ultrasonic intrusion detectors is described. This simulator is primarily intended for use in environmental chambers to determine the effects of temperature and humidity on the operation of ultrasonic intrusion detectors.

DISCLAIMER

This document contains information which is classified as "Confidential" by the United States Government. Neither the United States Government nor any agency thereof, nor any other individual, firm, or organization, makes any warranty, expressed or implied, or assumes any legal liability or responsibility for the accuracy, completeness, or usefulness of any information, apparatus, product, or process disclosed, or represents that its use would not infringe privately owned rights. Reference herein to any specific commercial product, process, or service by trade name, trademark, manufacturer, or otherwise, does not necessarily constitute or imply its endorsement, recommendation, or approval by the United States Government or any agency thereof. The views and opinions of authors do not necessarily state or reflect those of the United States Government or any agency thereof.

DISTRIBUTION OF THIS DOCUMENT IS UNLIMITED

89

ACKNOWLEDGMENT

The design and development of the ultrasonic intruder simulator and text preparation were performed by D. C. Miller. M. K. Bumgardner assisted in text preparation and application of the intruder simulator. The text was critically reviewed and edited by R. D. Williams and M. K. Bumgardner. This work was sponsored by the U.S. Department of Energy, Office of Safeguards and Security (DOE/OSS).

CONTENTS

<u>Section</u>		<u>Page</u>
1	INTRODUCTION	7
2	INTRUDER DETECTION THEORY	9
	2.1 Evaluation Approach	9
	2.2 Principles of Operation and Test Parameters	9
3	ELECTRONIC SIMULATION	13
4	SYSTEM DESCRIPTION	15
	4.1 System Hardware	15
	4.2 System Operation	17
	4.3 Software Description	21

ILLUSTRATIONS

<u>Figure</u>		
1	The Principle of Monostatic Doppler Motion Detectors	10
2	Spherical Coordinate System Used in This Evaluation	11
3	Automat. Ultrasonic Intruder Simulator Electronic Hardware	15
4	Ultrasonic Intruder Temperature Chamber Hardware	16
5	Ultrasonic Intruder Temperature Chamber Hardware--Pseudo-Anechoic Chamber	17
6	Ultrasonic Intruder Temperature Chamber Hardware--Barrel with Acoustic Absorber	18
7	Automated Ultrasonic Intruder Simulator Flow Chart	19
8	A.D.L. Series 77 Plot	29
9	Advisor VI Plot	21
10	Program No. 1 Listing	22
11	Program No. 1 Flow Chart	22
12	Program No. 2 Listing	23
13	Program No. 2 Flow Chart	24
14	Program No. 3 Listing	26
15	Program No. 3 Flow Chart	26
16	Program No. 4 Listing	27
17	Program No. 4 Flow Chart	27
18	Program No. 5 Listing	28
19	Program No. 5 Flow Chart	30
20	Program No. 6 Listing	34
21	Program No. 6 Flow Chart	35
22	Program No. 7 Listing	36
23	Program No. 7 Flow Chart	37
24	Program No. 8 Listing	39
25	Program No. 8 Flow Chart	40

TABLE

Table

I

Program Running Order

Page

21

AN AUTOMATED ELECTRONIC INTRUDER SIMULATOR
FOR EVALUATION OF ULTRASONIC INTRUSION DETECTORS

1. INTRODUCTION

Ultrasonic intrusion detectors are often installed at Department of Energy (DOE) sites inside buildings that have no heating or air-conditioning systems. As a consequence, these units are frequently subjected to temperature and humidity extremes.

This report describes an ultrasonic electronic intruder simulator which will be used in environmental chambers to test the effects of temperature and humidity on the electronic and transducer components of ultrasonic intrusion detectors. The radius of detection of the intrusion detectors for radial intruder velocities which range from 0.1 m/s to 4 m/s will also be measured by the simulator to determine detection performance degradation. The simulator reproduces the motion and position of the intruder by injecting a Doppler shift (a function of the radial velocity of the intruder) at a given power level (a function of the radial distance to the intruder) into the sensor circuit at the point in the circuit where the output from the sensor detector would normally appear. The following discussion develops the mathematics associated with this simulation and outlines a simple calibration technique that relates the data obtained with the simulator to the data obtained with an actual intruder.

2. INTRUDER DETECTION THEORY

2.1 EVALUATION APPROACH

The automated electronic intruder simulator can be used to evaluate monostatic (receiver and transmitter at same location) motion detectors which detect the Doppler shift produced by reflections from moving intruders. This type of system can be used in rooms of various types and sizes. Since detection is based on line-of-sight criteria, the radar-range detection evaluation approach can be used.*

The methods used for evaluating motion detection characteristics are mainly walk-tests. These walk-tests are done in a large open room, approximately 16 by 16 by 3.6 metres, to determine detection patterns, velocity factors, and range setting effects on the detection pattern. Radial detection patterns are also determined by electrically measuring the transmitted power patterns. Temperature effects are grossly determined at -15° C and 60° C by walk-tests. In order to allow a more comprehensive evaluation of temperature effects to be obtained, an electronic simulation is used which simulates the intruder by injecting, at the receiver, an electromagnetic signal which is proportional to the intruder's velocity toward and distance from the sensor.

2.2 PRINCIPLES OF OPERATION AND TEST PARAMETERS**

The operational principle of a monostatic motion detector that uses a Doppler shift to detect intruder movement is illustrated in Figure 1. These types of detectors are similar to conventional radar systems in that radar-range equations are applicable. However, motion detectors use continuous-wave signals and frequency-modulation detectors to detect Doppler shifts.

The far-field transmitted power density, P_T , in watts/metre² (W/m²), of the radiated signal measured at the intruder position (R, ϕ , θ) at the center frequency of the detector, f_0 , is given by

$$P_T(R, \phi, \theta) = \frac{P_T(1, 0, 90) G_R(\phi, \theta)}{R^2} \quad \text{for } R \geq 1.0 \text{ metre} \quad (1)$$

*The transmitted power in a wave varies as $1/R^2$ referenced to the transmitter; the wave is reflected from an intruder, and this reflection varies as $1/R^2$ referenced to the intruder.

**This section closely follows the corresponding section of SAND77-1218, Evaluation of Three Multi-Transceiver Ultrasonic Intrusion Detectors--Advisor VI, Contronic MD 440, and Detection Systems DS-600, June 1978.

where

- (R, ϕ, θ) = location of the intruder in spherical coordinates (see Figure 2), R is in metres, ϕ and θ are in degrees,
 $P_T(1, 0, 90)$ = reference power-density measurement at 1 metre (W/m^2),
 $G_T(\phi, \theta)$ = power gain associated with the transmitter transducer referenced to the $(0, 90)$ location (see Figure 2), and
 $P_T(R, \phi, \theta)$ = transmitted power density at the intruder location (W/m^2).

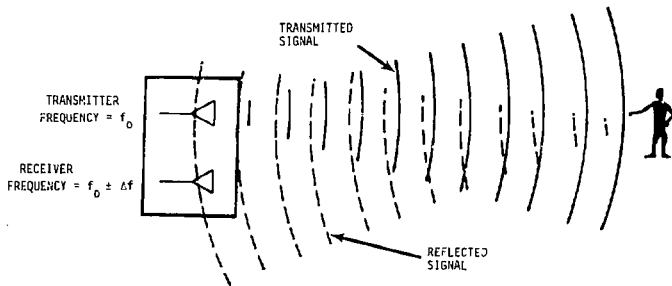


Figure 1. The Principle of Monostatic Doppler Motion Detectors

The transmitted power is reflected by the effective cross section of the intruder and returned to the receiver at a frequency of $f_0 \pm \Delta f$. The power at the receiver transducer terminals of the reflected signal is given by

$$P_R(0, \phi, \theta) = \frac{P_T(R, \phi, \theta) A G_R(\phi, \theta) \lambda^2}{(4\pi R)^2} \quad (2)$$

where

- A = effective reflective area of the intruder (m^2), assumed constant over the bandwidth of a particular system,
 $G_R(\phi, \theta)$ = power gain associated with the receiver referenced to the $(0, 90)$ location, and
 λ = wavelength of f_0 (metres).

Note that the Doppler shift and the radial velocity component of the intruder are related by

$$\Delta f \approx \frac{2f_0 V_r}{c} \quad (3)$$

where

c = wave propagation velocity (3×10^8 m/s microwave or 344 m/s ultrasonic)

V_r = radial velocity component of intruder (m/s), and

f_0 = transmitter center frequency.

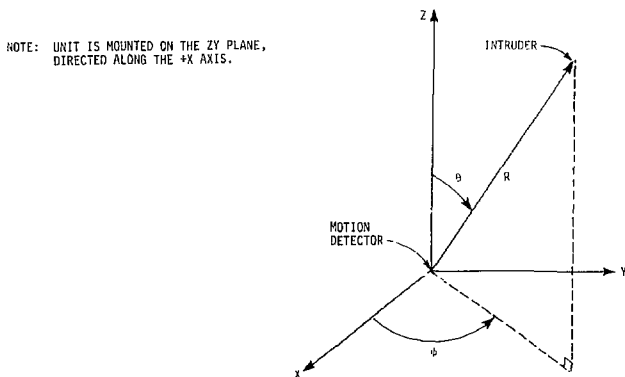


Figure 2. Spherical Coordinate System Used in This Evaluation

Combining Eqs. 1 and 2 yields

$$P_R(\theta, \phi, \theta) = \frac{P_T(1, 0, 90) A_G(\phi, \theta) G_R(\phi, \theta) \lambda^2}{(4\pi)^2 R^4} \quad (4)$$

There is a threshold value of P_R which, if exceeded for a short time, will trigger the alarm of the detector. This threshold determines the maximum radius of detection for a given set of intruder conditions (intruder area A , location (R, ϕ, θ) , and radial velocity V_r). Thus,

$$P_{RD}(\theta, \phi, \theta) = \frac{P_T(1, 0, 90) A_G(\phi, \theta) G_R(\phi, \theta) \lambda^2}{(4\pi)^2 R_D^4} \quad (5)$$

where

$P_{RD}(0, \phi, \theta)$ = detector power-density alarm threshold for a given Δf ; R_D is the radius of detection at the location of the intruder where $P_R = P_{RD}$.

The radius of detection is

$$R_D = \left[\frac{P_T(1, 0, 90) A G_T(\phi, \theta) G_R(\phi, \theta) \lambda^2}{(4\pi)^2 P_{RD}(0, \phi, \theta)} \right]^{1/4} \quad (6)$$

3. ELECTRONIC SIMULATION

In environmental tests, the radius of detection as a function of intruder radial velocity is measured at several different temperatures and one sensitivity setting. In Eq. 6, $\theta = 90^\circ$ and $\gamma = 0^\circ$ (radial intruder motion).

Note that R_D and P_{RD} are the only variables in Eq. 6; each is a function of intruder velocity. Thus,

$$R_D^4(V)P_{RD}(V) = K_1 \quad (7)$$

and

$$R^4(V)P_R(V) = K_1 \quad (8)$$

The electronic simulator must simulate the variable $P_R(V)$ when a voltage v is injected into the system.* Since power is proportional to voltage squared,

$$P_R(V) = K_2 v^2 \quad (9)$$

and

$$P_{RD}(V_1) = K_2 v_{RD}^2 \quad (10)$$

where

$$v_{RD} = \text{alarm threshold voltage.}$$

For calibration purposes, the detector is walk-tested at a velocity V_1 and the radius of detection, $R_D(V_1)$, is measured. In this case,

$$K_1 = R^4(V)K_2V^2 \quad (11)$$

$$K_1 = R_D^4(V_1)P_{RD}(V_1) \quad (12)$$

*Voltage is easily programmed and monitored with the HP9825A calculator/controller.

$$K_1 = R_{D_1}^4(V_1) K_2 v_{RD}^2(V_1) \quad (13)$$

Combining Eqs. 11 and 13 yields

$$v(V) = \frac{R_D^2(V_1) v_{RD}(V_1)}{R^2(V)} \quad (14)$$

or

$$v(V) = \frac{R_D^2(V_1) v_{RD}(V_1)}{(K_3 - V\Delta t)^2} \quad (15)$$

where

$$R = K_3 - V\Delta t$$

K_3 = the range at which the unit does not detect, $\approx 1.5 R_{MAX}$,

V = intruder velocity (m/s),

Δt = elapsed time from the start position.

Thus, the electronic simulator starts the intruder at a distance approximately 1.5 times the maximum range of the unit and increases power to the receiver at a rate and frequency shift which correspond to the intruder velocity. For calibration purposes, the values of V_1 , R_{MAX} , and $R_D(V_1)$ are determined manually. The value of $v_{RD}(V_1)$ is then obtained by gradually incrementing the voltage to the simulator transducer at a Doppler which corresponds to the velocity V_1 . Eq. 6 is now a function of the intruder velocity, V , and radius, R ; all other parameters are known.

4. SYSTEM DESCRIPTION

4.1. SYSTEM DESCRIPTION

A photograph of the automated ultrasonic intruder simulator electronic hardware is shown in Figure 3. The heart of the simulator is an HP9825A calculator controller. By use of proprietary software, the HP9825A enables the operator to control and collect data from various instruments which are input to an interface bus. The basic computer equipment used in the simulator includes an HP3455A digital multimeter, HP1040B logic programmer, an HP53287 universal counter, and a HP9845A plotter. Equipment which is not connected to the bus includes a Tektronix 335 oscilloscope, an HP467A power amplifier, a 100 watt power supply, a 10X attenuator, a coax switching panel, a B&K Type 143 amplifier, a B&K Type 4113 microphone, a speaker, a General Eastern 400C/D temperature humidity indicator with probe, and a "pseudo-echoic" chamber.

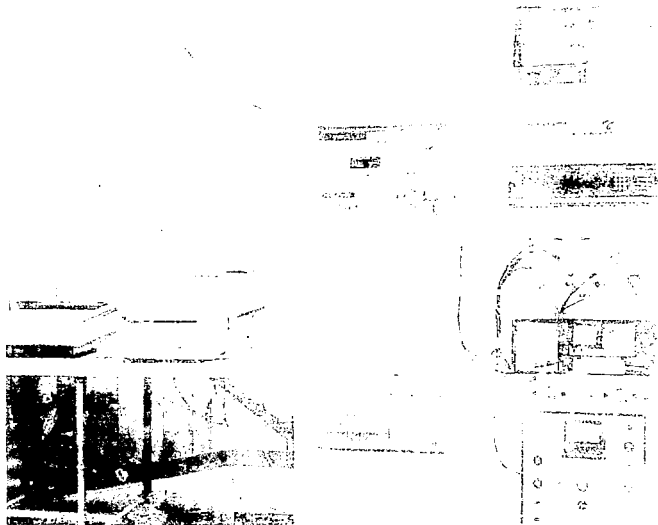


Figure 3. Automated Ultrasonic Intruder Simulator Electronic Hardware

Tests are normally performed within one of two environmental chambers: a hot chamber and a cold chamber (shown in Figure 4). Temperature is held at 100° to -20° C to ambient in the cold chamber and the ambient level in the hot chamber. However, the circulating fans and the highly reflective walls of the chambers can produce unwanted sensor stimuli.

Therefore, a pseudo-anechoic chamber (shown in Figure 5) was developed and effectively protects the sensor from external stimuli, with the exception of true temperature effects. The sensor, which is mounted on the end of the barrel, is surrounded with acoustic absorber, faces a barrel open on one end and closed on the other with acoustic absorber (see Figure 6). A speaker and microphone are located symmetrically in the closed end of the barrel.



Figure 4. Ultrasonic Intruder Temperature Chamber Hardware

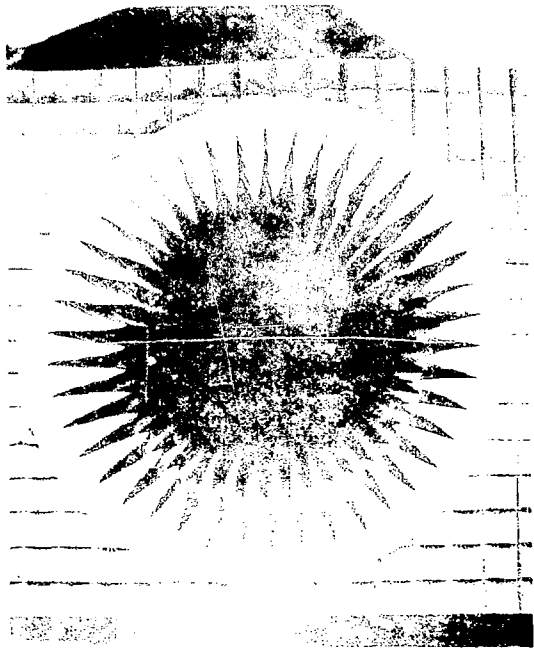


Figure 7. Harmonic Generator Output

A flow chart of the operation of the harmonic generator is shown in Figure 7. Initially, a sample is placed in the harmonic generator. The HP467A power amplifier is used to drive the input of the NFM generator matches the specific needs of the sample being analyzed.

The General Eastern 4502 harmonic generator has a dc output voltage proportional to the temperature of the sample. This voltage is measured by the H4430 digital voltmeter. The data is sent to the P9825A calculator/controller.

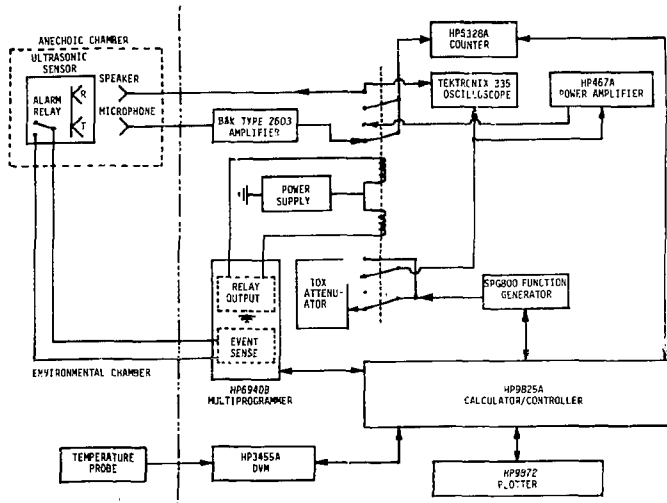


Figure 7. Automated Ultrasonic Intruder Simulator Flow Chart

To begin the main portion of the program, the B&K 2603 microphone samples the transmitted signal of the ultrasonic sensor. This signal is amplified by the B&K 2603 amplifier, and then its frequency is measured by the HP5328A universal counter. This information is then sent to the HP9825A calculator/controller.

When the environmental chamber reaches the temperature specified in the program, the HP9825A takes the sensor transmitted frequency and adds to it the first of nine preselcted Doppler shifts. This new frequency is then programmed into the SPG800 function generator. At this time, a number of operations are performed by the HP9825A almost simultaneously. The event-sense card of the HP6940B multiprogrammer is enabled. An initial signal amplitude (calculated with the test parameters described in Section 2.2) is programmed into the SPG800 generator. The HP5328A universal counter is programmed to act as a timer and is started at $T = 0$. A relay on the relay output card is activated, closing a coax switch. This closure allows the shifted signal to pass through the 10X attenuator and the HP467A power amplifier into the speaker.

According to the test parameters given in Section 2.2, the amplitude of the signal is stepped up with respect to time until either an alarm occurs or the

voltage is equal to 10. If the voltage becomes equal to 10, another relay on the relay output card is activated, closing another coax switch and disabling the 10X attenuator. The signal amplitude is immediately divided by 10 but continues to rise, in accordance with Eq. 6, until an alarm occurs or voltage = 16 (the limit of the SPG800).

If no alarm occurs, this is noted. If an alarm occurs, the amplitude of the signal as well as the elapsed time are stored and processed according to the parameters contained in Section 2. After a 30-second wait, the process is begun again using the next Doppler shift. When the last Doppler is complete, the program outputs the data. If the test being performed is the ambient test, the program then terminates; otherwise, it waits for the next 6° C temperature change to occur and then begins the testing sequence again.

As each temperature section of the program is completed, the data are graphically output by the HP9872A plotter. Two example plots are shown in Figures 8 and 9. The horizontal scale is a logarithmic scale of the velocities which correspond to the injected Dopplers. The vertical scale represents the detection range normalized to 1.

If the test being performed is the first one for a particular sensor or if the power output of the sensor transmitter has changed due to temperature effects, a calibration will be initially required. The calibration described in Section 2

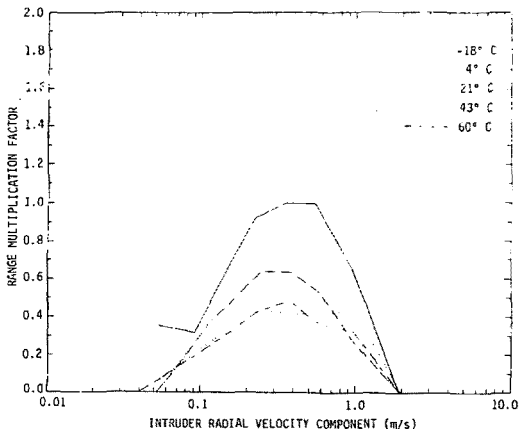


Figure 8. A.D.L. Series 77 Plot

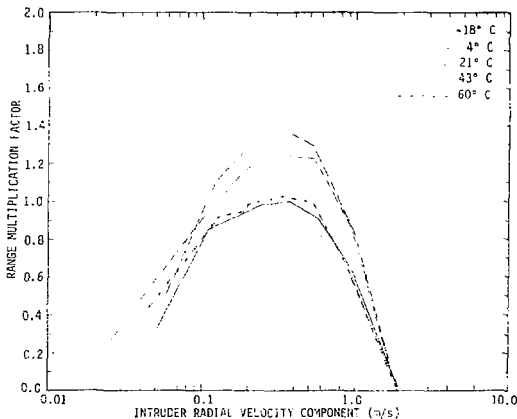


Figure 9. Advisor VI Plot

is performed in a similar manner. The Doppler frequency determined by the walk-test is injected into the speaker at a very small amplitude. The amplitude is gradually increased until an alarm occurs. The final amplitude is stored, and the program continues into the main body.

4.3 SOFTWARE DESCRIPTION

The control for the automated ultrasonic intruder simulator consists of eight programs written in H.P.L. (Hewlett Packard Language). The programs are assembled and run according to the requirements input to the HP9825A by the operator. Table I shows the running order of the programs. Figures 10 through 25 show the program listing and associated flow chart for each of the eight programs.

TABLE I
Program Running Order

Type of <u>Environmental Test</u>	Calibration <u>Required?</u>	Programs Run <u>(in order)</u>
Ambient	Yes	1-2-5-6
High temperature	Yes	1-2-3-5-7
High temperature	No	1-3-5-7
Low temperature	Yes	1-2-4-5-8
Low temperature	No	1-4-5-8

```

0: clr 7;fxd 0;fmt 1,c,z
1: dim AS[15],BS[10],CS[15],DS[24],E[10],F[10]
2: dim KS[30],GS[10,10]
3: ent "SENSOR UNDER TEST?" ,KS
4: ent "CENTER VELOCITY?" ,P
5: ent "MAXIMUM RANGE?" ,Q
6: ent "Vmin?" ,S
7: cmd 717,"B3KCIKD01KM0KH"
8: "F00000E4KA" -> AS
9: "00000E0K" -> CS
10: ent "TEST?: 1=AMBIENT,2=HOT,3=COLD",A
11: if S=0;ldf 2,11
12: if A=2;ldf 3,11
13: if A=3;ldf 4,11
14: end
*5094

```

Figure 10. Program No. 1 Listing

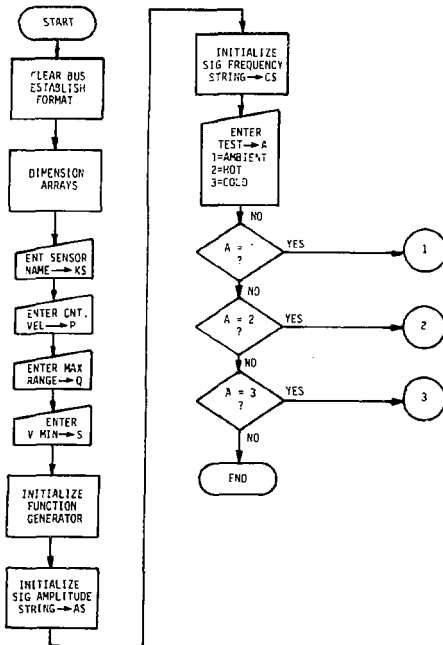


Figure 11. Program No. 1 Flow Chart

```

0: 0-F;1-X;1-M;0-N;10-E
1: clr 702
2: wrt 702,"PF4G0T"
3: red 702,0
4: str(B)-05
5: 2BP/344-X
6: val(B$[1,6])*X-D
7: str(0)-AS[2,6]
8: if E<100;3-H;jmp 4
9: if E<100;2+H;jmp 3
10: if E<100;1-H;jmp 2
11: if E>=100;end
12: str(E)+CS[H,5]
13: wait 3000
14: ASCS-D5
15: prt D5
16: cmd 717,N5
17: wrt 723.1,"00040TG0001T"
18: rds(723)+C;oni 7,"interrupt"
19: wrt 723.1,"00040TC7777T"
20: wrt 723.1,"0020TC0040T";eir 7
21: wait 5000
22: if flg1;jmp 7
23: "interrupt":if rds(723)#64;gto "iret"
24: wrt 723.1,"00040TC7777T"
25: sfg 1
26: wrt 723.1,"00040TG0000T";wait 500
27: "iret":iret
28: E+10-E;wrt 723.1,"00040TG0000T";wait 1000;jmp -20
29: fxd 0;.1E-5;prt 5;wait 5000
30: fxd 2;1-x;1-y;eir 7,2
31: if A=1;ldf 5,42
32: if A=2;ldf 3,42
33: if A=3;ldf 4,42
*7061

```

Figure 12. Program No. 2 Listing

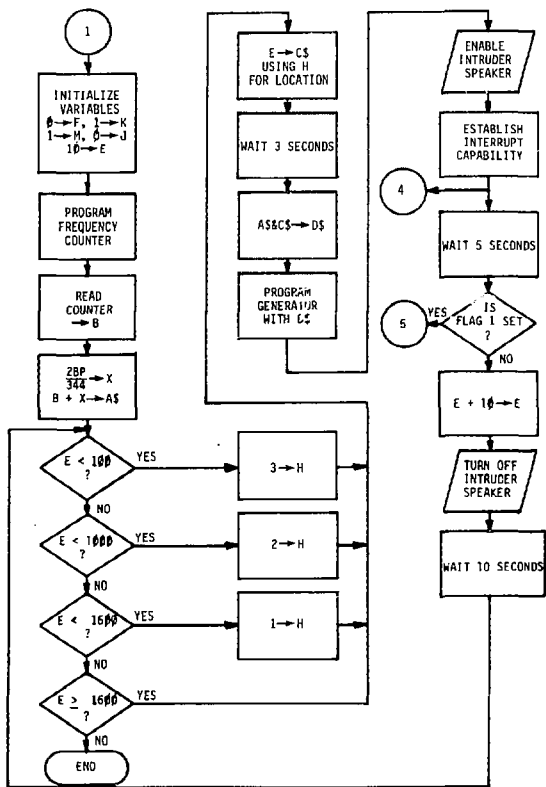


Figure 13. Program No. 2 Flow Chart

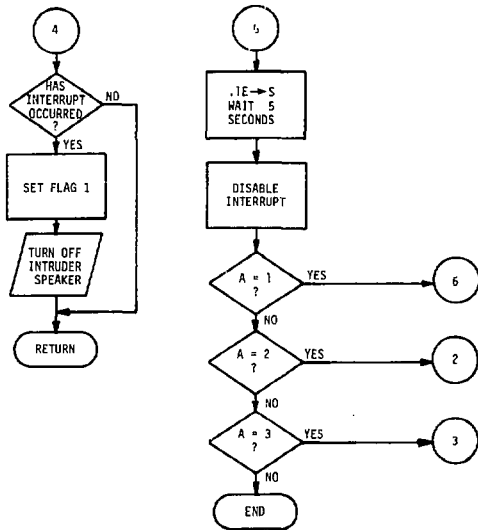


Figure 13. Continued

```

0: 0←1;150←U;0←W
1: "TEMP":fxd 2;1←X;1←N;efr 7,0;1←1;U-10←U;0←F;1←K;1←M
2: wrt 722,"F1R4A1H00IM3T3E"
3: trg 722
4: rcd 722,Y;(Y+.06)20←Y
5: if Y<=U;jmp 2
6: jmp -3
7: ldf 5,1B
*23572

```

Figure 14. Program No. 3 Listing

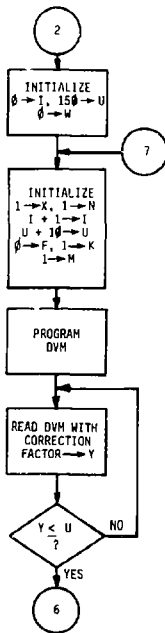


Figure 15. Program No. 3 Flow Chart


```

0:  $\beta \rightarrow I; -1\beta \rightarrow U; \beta \rightarrow W$ 
1: "TEMP":fxd 2;l>X;1-N;eir 7,0;1+1+I;U+10+U; $\beta \rightarrow F$ ;1-K;1-M
2: wrt 722,"FIR4A1H00INST3E"
3: trg 722
4: rdg 722,Y;(Y+.06)20-Y
5: if Y>=U;jmp 2
6: jmp -3
7: ldf 5,18
*2344 $\beta$ 

```

Figure 16. Program No. 4 Listing

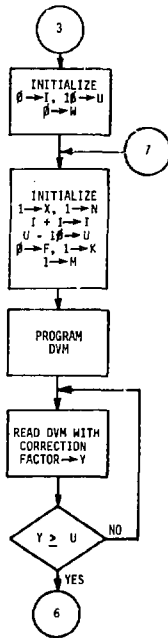


Figure 17. Program No. 4 Flow Chart

```

0: 0-J;1.5Q-R;0300"-CS(1,5)
1: fxd 0:c1r 702
2: wrt 702,"PF4G5T";wait 500
3: read 702,B;str(B)-05
4: prt B
5: fxd 0
6: val(BS[1,5])*X-0
7: prt 0
8: 10D-B-X
9: fxd 2
10: 344X/2B-V
11: prt V
12: fxd 0
13: str(D)-AS[2,6]
14: AS&CS-DS
15: cmd 717,DS
16: wrt 723.1,"00040TG00001T"
17: fxd 3;wrt 702,"PF1F2G4S5R"
18: if f1g1;jmp 20
19: if R<-1;jmp 26
20: S(Q/R)+2-E;dsp E
21: E=T
22: if E>1000;E/10+E
23: if E<9.5;4-H;jmp 5
24: if E<9.5;3+H;jmp 4
25: if E<999.5;2+H;jmp 3
26: if E<1600;1+H;jmp 2
27: if E=>1600;jmp 18
28: str(E)-CS[H,5]
29: AS&CS-DS
30: cmd 717,DS
31: if T>1000;wrt 723.1,"00040TG00003T"
32: rds(723)-C;ont 7,"inter"
33: wrt 723.1,"00040TC7777T"
34: wrt 723.1,"00240TC02460T";eir 7
35: eir 7,0
36: red 702,G;G/10+7+G;G-J-2;G+J
37: R-ZV+R
38: jmp -20
39: "inter":if rds(723)#64;gto "iret"
40: wrt 723.1,"00040TC7777T"
41: wrt 702,"F055"
42: sfg 1;17000-E;.01-R
43: wrt 723.1,"00040TG00000T";wait 5000
44: "iret":iret
45: eir 7,0;ctg ;if A=0;F+1-F;0=E[F];wrt 702,"F055";"NO ALARM"-GS[F];jmp 3
46: eir 7,0;ctg ;F+1-F;fxd 2;str(T/1000)-GS[F];fxd 0
47: r{(1/T)-E[F]}
48: log(344X/2B)-F[F]
49: if F<4;N+1-N;N-X
50: if F=4;6-X
51: if F=5;9-X
52: if F=6;15-X
53: if F=7;30-X
54: if F=8;60-X
55: wrt 723.1,"00040TG00001T"
56: if F=9;jmp 2
57: wait 30000;jmp -56
*22667

```

Figure 18. Program No. 5 Listing

```

58: max(E[*])-J
59: if I>1;jmp 14
60: fxd 0
61: pctr;tb1 " "
62: pen# 1
63: scl -2.5,2,-.2,1
64: xax 0.1,-2.1,10
65: fxd 1
66: yax -2.1,0.1,2
67: plt -1.65,-.1,1;tb1 "LOG[INTRUDER RADIAL VELOCITY COMPONENT(m/sec)]"
68: csiz 1.5,2,1.90
69: plt -2.3,.22,1;tb1 "RANGE MULTIPLICATION FACTOR"
70: csiz 2.5,2,2/3,0
71: -.5-(len(K$)/2).0428-Y
72: plt Y,-.19,1;tb1 K$
73: if A=1;ldf 6,115
74: if A=2;ldf 7,91
75: if A=3;ldf 8,91
*25987

```

Figure 18. Continued

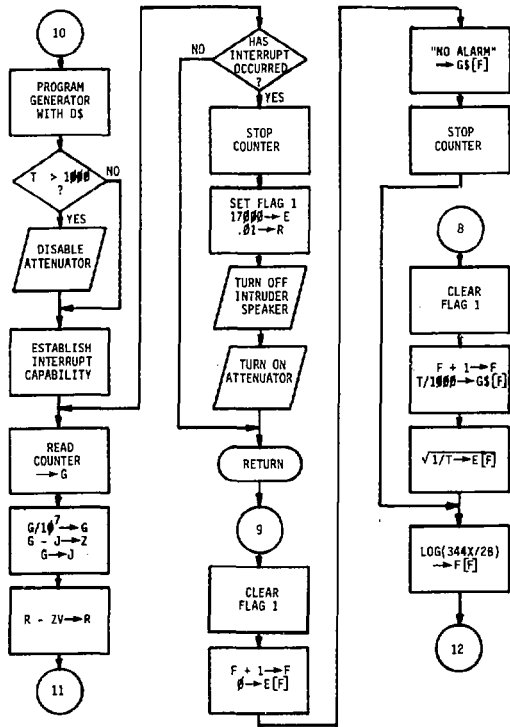


Figure 19. Continued

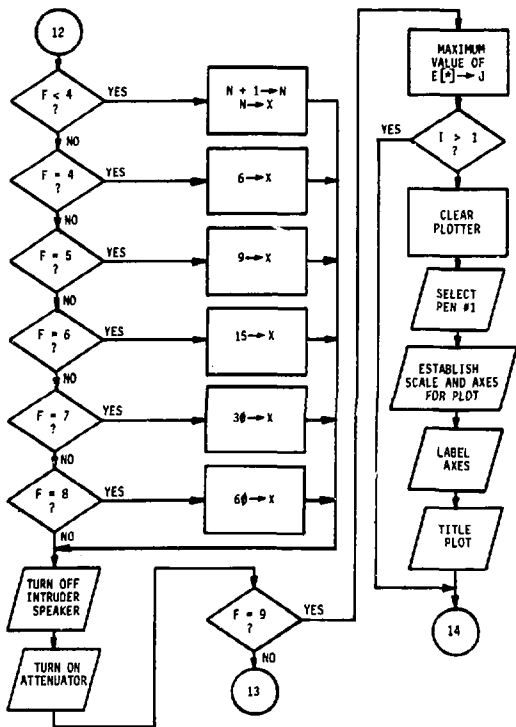


Figure 19. Continued

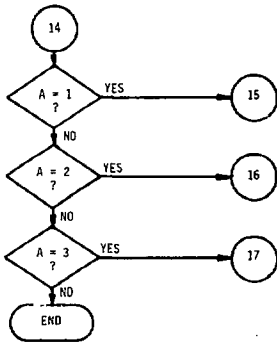


Figure 19. Continued

```

0: plt 1.2,.88,1
1: plt 1.93,.88,2
2: plt 1.48,.96,1
3: plt 1.48,0,2
4: csiz 1.5,2,1,0
5: plt 1.2,.94,1;|b1 "DATA ALARM"
6: plt 1.2,.89,1;|b1 "POINT VOLTAGE"
7: fxd 3
8: T[S/1000/16]-Z
9: line 6
10: plt -2,Z,i
11: plt 1,Z,2
12: line
13: E[K]/J+L
14: plt F[K],L,M
15: fxd 0
16: |b1 K
17: plt F[K],L,-2
18: K+I+K;0-M
19: if K>S,jmp 2
20: jmp -7
21: L+K,85+N
22: plt 1.25,N,1;|b1 K;fxd 2;|b1 " " ,GS[K]
23: N-.03-N;K+I-K;fxd 0
24: if K>S;pene ;end
25: jmp -3
*29762

```

Figure 20. Program No. 6 Listing

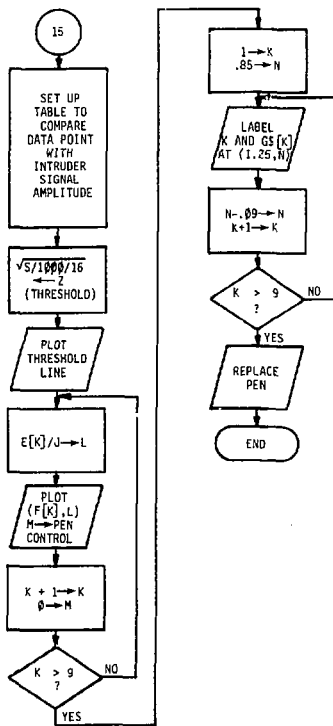


Figure 21. Program No. 6 Flow Chart

```

0: csiz 1.5,2,1,0
1: if I=1;pen# 2;plt 1,.9,1;plt 1.5,.9,2;tbl "140deg.F.";jmp 3
2: W+1-W
3: line W
4: if I=2;pen# 3;plt 1,.8,1;plt 1.5,.8,2;tbl "130deg.F."
5: if I=3;pen# 4;plt 1,.7,1;plt 1.5,.7,2;tbl "120deg.F."
6: if I=4;pen# 1;plt 1,.6,1;plt 1.5,.6,2;tbl "110deg.F."
7: if I=5;pen# 2;plt 1,.5,1;plt 1.5,.5,2;tbl "100deg.F."
8: if I=6;pen# 3;plt 1,.4,1;plt 1.5,.4,2;tbl " 90deg.F."
9: if I=7;pen# 4;plt 1,.3,1;plt 1.5,.3,2;tbl " 80deg.F."
10: E(K)/J-L
11: plt F(K),L,M
12: fxd 0
13: tbl K
14: plt F(K),L,-2
15: K-I-K;0-M
16: if K>9;jmp 2
17: jmp -7
18: pen# ;line
19: if I>=7;end
20: gto "TEMP"
*23126

```

Figure 22. Program No. 7 Listing

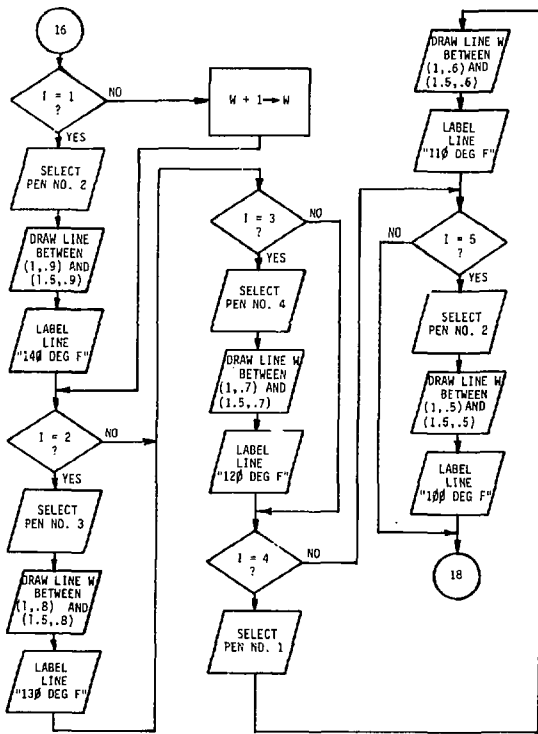


Figure 23. Program No. 7 Flow Chart

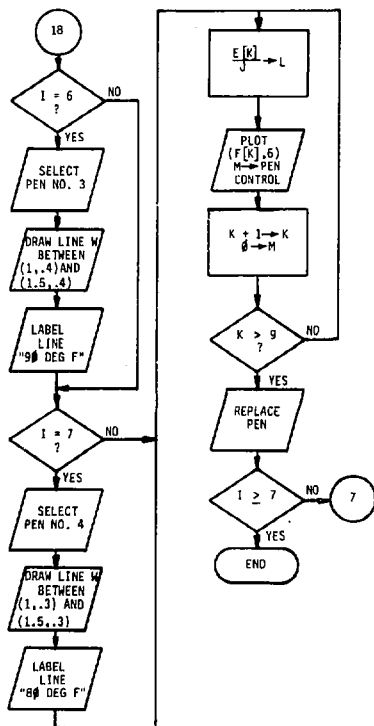


Figure 23. Continued

```

0: csiz 1.5,2,1,0
1: if l=1;pen# 2;plt 1.9,1;plt 1.5,.9,2;lbl " 0deg.F.";jmp 3
2: W+1-W
3: line W
4: if l=2;pen# 3;plt 1.8,1;plt 1.5,.8,2;lbl "10deg.F."
5: if l=3;pen# 4;plt 1.7,1;plt 1.5,.7,2;lbl "20deg.F."
6: if l=4;pen# 1;plt 1.6,1;plt 1.5,.6,2;lbl "30deg.F."
7: if l=5;pen# 2;plt 1.5,1;plt 1.5,.5,2;lbl "40deg.F."
8: if l=6;pen# 3;plt 1.4,1;plt 1.5,.4,2;lbl "50deg.F."
9: if l=7;pen# 4;plt 1.3,1;plt 1.5,.3,2;lbl "60deg.F."
10: E(K)/J+L
11: plt F[K].L,M
12: rxd 0
13: lbl K
14: plt F[K].L,-2
15: K+1+K;0+M
16: if K>9;jmp 2
17: jmp -7
18: pen# ;line
19: if l>=7;end
20: gto "TEMP"
*21652

```

Figure 24. Program No. 8 Listing

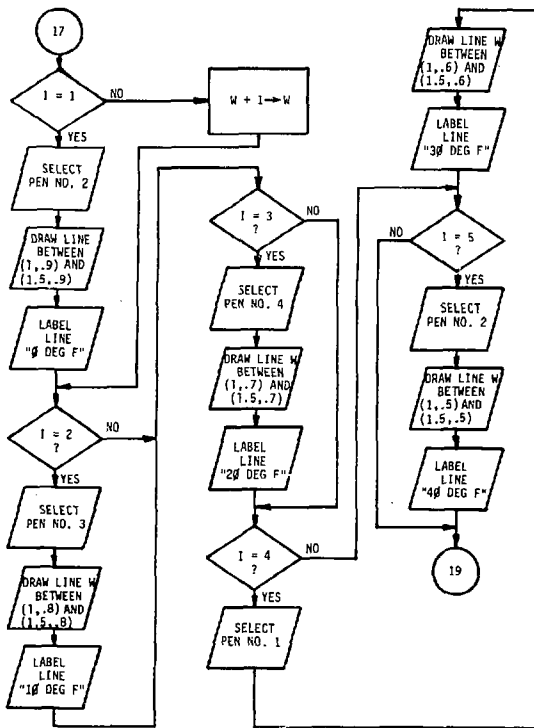


Figure 25. Program No. 8 Flow Chart

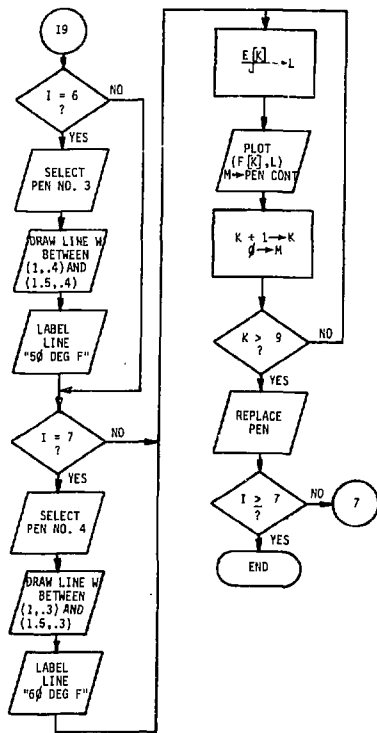


Figure 25. Continued